ELSEVIER

Biophysical Chemistry 72 (1998) 185–200

Biophysical Chemistry

Mathematical model of the fission yeast cell cycle with checkpoint controls at the G1/S, G2/M and metaphase/anaphase transitions

Bela Novak[a,*], Attila Csikasz-Nagy[a], Bela Gyorffy[a], Kathy Chen[b], John J. Tyson[b]

[a]*Department of Agricultural Chemical Technology, Technical University of Budapest, Gellert ter 4, Budapest 1521, Hungary*
[b]*Department of Biology, Virginia Polytechnic Institute and State University, Blacksburg, VA 24061, USA*

Revision received 16 January 1998; accepted 13 February 1998

Abstract

All events of the fission yeast cell cycle can be orchestrated by fluctuations of a single cyclin-dependent protein kinase, the Cdc13/Cdc2 heterodimer. The G1/S transition is controlled by interactions of Cdc13/Cdc2 and its stoichiometric inhibitor, Rum1. The G2/M transition is regulated by a kinase-phosphatase pair, Wee1 and Cdc25, which determine the phosphorylation state of the Tyr-15 residue of Cdc2. The meta/anaphase transition is controlled by interactions between Cdc13/Cdc2 and the anaphase promoting complex, which labels Cdc13 subunits for proteolysis. We construct a mathematical model of fission yeast growth and division that encompasses all three crucial checkpoint controls. By numerical simulations we show that the model is consistent with a broad selection of cell cycle mutants, and we predict the phenotypes of several multiple-mutant strains that have not yet been constructed.

Keywords: Size control; Start; Cyclin-dependent kinase; Anaphase promoting complex; Rum1; Wee1; Cdc25

1. Introduction

The fundamental process underlying all biological growth and reproduction is the cell division cycle: the sequence of events whereby a living cell duplicates its essential components and distributes them at division to two daughter cells, which are capable of repeating the sequence themselves. Most components of a cell, such as ribosomes, membranes, and housekeeping enzymes, are present in large quantities or they may be synthesized de novo from other components, so their exact partitioning between daughter cells is not crucial. But some essential, self-replicating components (notably, chromosomes and spindle pole bodies) are present in only two copies at division, so they must be precisely replicated during the cell cycle and accurately partitioned at division. Elaborate control mechanisms over DNA synthesis and mitosis ensure that these crucial events of the cell cycle are carried out properly.

In most eukaryotic cells this coordination of events is carried out at three 'checkpoints' [1]. A checkpoint is a stage of the cell cycle where progress is halted until certain 'surveillance mechanisms' relay signals that conditions are suitable for resuming progress through the cycle. For instance, in G1-phase, cells scrutinize their external environment (for nutritional conditions, growth factors, pheromones, etc.) and

* Corresponding author. E-mail bnovak@chem.bme.hu

0301-4622/98/$19.00
PII S0301-4622(98)00133-1

their internal state (nucleocytoplasmic ratio) before committing to a new round of DNA synthesis and division. In G2-phase, before initiating the mitotic process, cells check that DNA synthesis and repair are complete and that cell size is large enough. At metaphase, they ensure that all chromosomes are properly aligned on the metaphase plate before issuing the command to segregate sister chromatids to opposite poles of the mitotic spindle.

In recent years many of the molecular details of these control mechanisms have been uncovered by the powerful techniques of molecular genetics. The controls revolve around cyclin-dependent protein kinases (CDKs) which trigger the major events of the eukaryotic cell cycle. For instance, when all requirements of the G1 checkpoint are satisfied, activation of a specific cyclin/CDK dimer initiates DNA synthesis at numerous origins of replication on the chromosomes. When the G2 checkpoint is lifted, a different cyclin/CDK dimer drives the cell into mitosis. At metaphase, when all chromosomes are properly aligned, the cell activates a specific proteolytic pathway that degrades certain centromeric proteins and mitotic cyclins, inducing sister chromatid separation and nuclear division. Although the molecular interactions regulating CDK activities are known in great detail, the mechanisms of the checkpoint controls are still uncertain.

Mathematical models of cell cycle controls have kept pace with the advances of molecular genetics [2–5]. In these models, biochemical mechanisms are translated, by the law of mass action, into systems of non-linear differential equations, and dynamical systems theory is used to uncover the qualitative behavior of these equations and to bridge the gap between mechanisms and physiology. From a mathematical point of view, the cell biologist's notion of a 'checkpoint' can be interpreted as a 'stable steady state solution' of the differential equations, and these checkpoints are imposed and lifted by bifurcations that create and destroy stable steady states [3,5,6]. 'Surveillance mechanisms' transduce intracellular or extracellular signals into changes (usually post-translational) in the regulatory enzymes of the CDK network, thereby inducing parameter variations that impose and lift checkpoints. Adopting this point of view, we present a simple, dynamical model of the three checkpoint controls in fission yeast.

2. Cell cycle controls in fission yeast

Fission yeast (*Schizosaccharomyces pombe*) is an attractive organism for studying eukaryotic cell cycle controls, and a wealth of information has been accumulated about its physiology, genetics and molecular biology [7]. Its cell cycle is controlled by a single CDK, namely Cdc2 (the protein encoded by the $cdc2^+$ gene), in combination with three B-type cyclins (Cdc13, Cig1, and Cig2; for review see Ref. [8]). The most important cyclin partner of Cdc2 protein is Cdc13. The complex of Cdc2 and Cdc13 (known as M-phase promoting factor (MPF)) is absolutely essential to initiate mitosis, and in the absence of other cyclins, this complex can trigger S-phase as well [9]. The Cdc13 level fluctuates dramatically during the cell cycle, reaching a maximum as cells enter mitosis, dropping precipitously as cells exit mitosis, and reappearing after S-phase is initiated [10]. The activity of Cig2-dependent kinase peaks at the G1/S transition [11,12], and it, together with Cdc13-dependent kinase, is responsible for S-phase initiation during normal cell cycles. Cig1-dependent kinase peaks at M-phase [13]; its physiological role is not known. In addition to the three B-type cyclins, fission yeast has a fourth cyclin with unknown function, Puc1 (for review see Ref. [8]), whose concentration is roughly constant (small compared with the Cdc13 level at mitosis) over the cell cycle [47].

Cdc2, the catalytic subunit of the heterodimer, is present at a constant level throughout the cell cycle. Its catalytic activity is determined not only by the availability of cyclin partners but also by phosphorylation at two specific amino acids: Thr-167 and Tyr-15 (for review see Ref. [14]). Phosphorylation of Thr-167, which is necessary for Cdc2 kinase activity, happens rapidly after cyclin binding and is not cell-cycle regulated. Tyr-15 phosphorylation, which inhibits Cdc2 kinase activity, is regulated: being high during S and early G2-phases and decreasing dramatically as cells enter M-phase. Phosphorylation of Tyr-15 is carried out by Wee1 and Mik1 kinases [15,16] and dephosphorylation by Cdc25 phosphatase [17,18].

Both Wee1 and Cdc25 are regulated in *Xenopus* oocytes by MPF-dependent phosphorylation (for review see Ref. [19]) and possibly the same is true in fission yeast [20,21]. Phosphorylation by active MPF inhibits Wee1 and activates Cdc25, and these

two positive feedback loops are responsible for the abrupt activation of MPF as cells enter M-phase.

In addition to cyclin availability and Cdc2 phosphorylation, cyclin/Cdc2 dimers can also be regulated by binding to inhibitory proteins. Nurse and co-workers [22,23] have identified Rum1 as a stoichiometric inhibitor of Cdc13/Cdc2 in fission yeast. Its level is high in G1, not detectable in S and G2, and rises again at the end of mitosis [23,47]). Cig2/Cdc2 complexes are also inhibited by Rum1, but not so much as Cdc13/Cdc2; whereas Cig1 and Puc1 complexes are insensitive to Rum1 [11,23,24].

2.1. G2 checkpoint

Wild type fission yeast cells have short durations of G1, S and M-phases, and a long G2-phase (Fig. 1A). Tyr-15 phosphorylation of Cdc2 is used to stop cells at the G2 checkpoint (see Ref. [25] for review). Two requirements must be met to start dephosphorylation of Tyr-15 residues: cells must reach a critical size and the chromosomal DNA must be fully replicated.

Comparing cells of different sizes at birth, Fantes [26] found that larger cells grow less during their division cycle (same growth rate but shorter cycle time), proving that cell size has a strong effect on progress through the cell cycle. Using nutritional shifts, Fantes and Nurse [27] proved that, in wild-type fission yeast, cells do not pass the size-control checkpoint until shortly before mitosis. Molecular genetics studies [15,17] implicated Cdc25 and Wee1 in the G2 size control mechanism. When cells are sufficiently large, the positive feedback loops engage, activating MPF and driving cells into mitosis [5].

The surveillance mechanism for unreplicated DNA also seems to work through Wee1 and Cdc25, by activating the phosphatase(s) opposing MPF-dependent phosphorylation of these enzymes [5]. As a consequence, MPF cannot turn on the positive feedback loops, and Cdc13/Cdc2 dimers are kept in their inactive, tyrosine-phosphorylated forms.

Novak and Tyson [5] have presented a thorough mathematical model of these G2 checkpoint mechanisms. The model compares favorably with many physiological and genetic studies of mitotic control in fission yeast.

2.2. G1 checkpoint

In *wee1*$^-$ mutants, Tyr-15 is not phosphorylated as normal and the G2 checkpoint malfunctions (see Ref. [14]). These mutants enter mitosis and subsequently divide at an abnormally small size [28]. They are small but viable, having a long G1-phase and short S + G2 + M (Fig. 1B). Immediately after division, *wee1*$^-$ cells are too small to enter S-phase; they must grow to a minimal size before they can leave G1 [29]. (Wild-type cells, on the

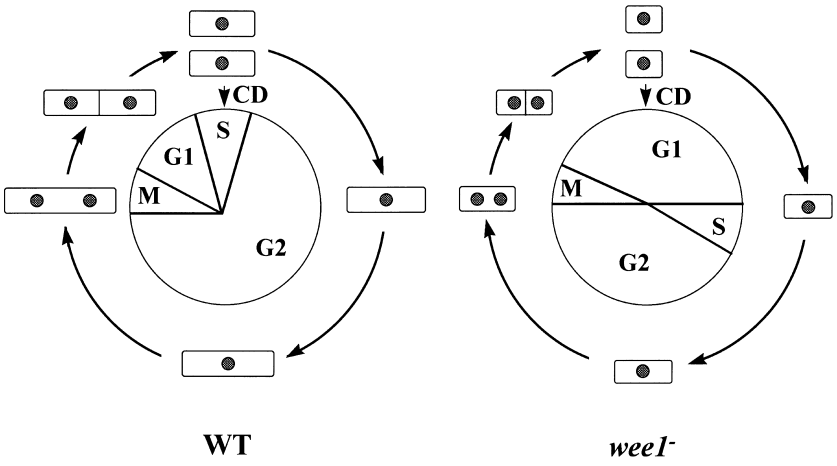

Fig. 1. The fission yeast cell cycle. (A) Wild-type cells. Approximate phase durations: G1 (15 min), S (10 min), G2 (90 min), M (5 min). Size at division: 14 μm. Size control operates in late G2-phase. (B) *wee1*$^-$ mutant cells. Phase durations: G1 (60 min), S (10 min), G2 (45 min), M (5 min). Size at division: 8 μm. Size control operates in late G1-phase.

other hand, are so large at mitosis that they can execute the G1/S transition quite soon after anaphase. To see the G1/S size requirement, cells must be born very small, either by wee mutations or by germination from spores).

The G1/S transition (Start) is controlled by antagonistic interactions between Rum1 and cyclin/Cdc2 dimers (Cig2/Cdc2 and Cdc13/Cdc2): Rum1 binds to and inhibits the dimers, whereas the dimers phosphorylate Rum1, making it more susceptible to proteolysis [47]. Below the critical size, Rum1 is predominant and progress through the cell cycle is stalled. Above the critical size, Rum1 inhibition is removed and cyclin/Cdc2 dimers drive the cell into S-phase. Recently, Novak and Tyson [30] have turned these ideas into a mathematical model, which can explain the behavior not only of *wee1*$^-$ (size control at Start), but also of *cdc13*Δ and *rum1*^{OP} (endoreplication) and *wee1*$^-$ *rum1*Δ (rapid division with diminishing cell size).

2.3. Mitotic checkpoint

At the end of mitosis, MPF is inactivated by degradation of its Cdc13 subunits. The degradation step is mediated by a multi-enzyme complex, called the anaphase promoting complex (APC), which attaches ubiquitin labels to cyclin molecules and renders them susceptible to proteolysis (for review see Ref. [31]). In addition to cyclin B molecules, the APC also induces degradation of the tether molecules that hold the sister chromatids together. The mitotic checkpoint ensures that APC is activated only after all chromosomes are properly attached to the bipolar mitotic spindle.

Two facts about the APC must be kept in mind. First, in frog egg extracts, for which normal checkpoint controls are inoperative, addition of active MPF can turn on cyclin degradation, but only after a significant time delay [32], suggesting that MPF activates (and/or induces production of) an intermediary protein that activates the APC. Second, APC activity and cyclin B accumulation seem to be mutually exclusive: in budding yeast [33] and fission yeast [34] the APC is active during G1-phase, when B-type cyclins are absent, and is inactive during S + G2 + M, when B-type cyclins are present. These facts led Nasmyth [44] to propose that cyclin B-dependent kinase activ-

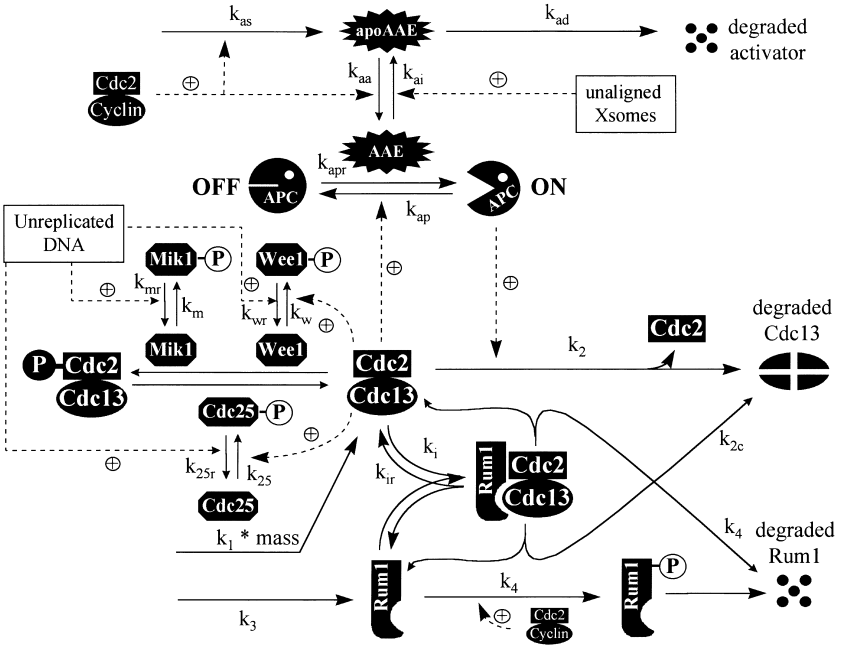

Fig. 2. A proposed molecular mechanism for three checkpoint controls in the fission yeast cell cycle. The G1/S transition is governed by CDK-Rum1 interactions; the G2/M transition by Wee1-Mik1-Cdc25-controlled tyrosine-phosphorylation of CDK; and the meta/anaphase transition by an 'APC activating enzyme' (AAE). See text for more details.

ity must be a potent inactivator of the APC as well. In support of this idea, Amon [35] has recently shown in budding yeast that artificially induced production of MPF in G1-arrested cells can turn off the APC, whereas MPF inhibition by overproducing Sic1 in S- or M-arrested cells can turn on the APC. Minshull et al. [36] have also suggested that MPF serves as both an activator and an inhibitor of cyclin B degradation.

In a recent paper, we envisioned a simple mechanism for the mitotic checkpoint [37]. The APC can exist in either an active or inactive form, and, to account for the mutual exclusion of MPF and APC activities, we assumed that MPF drives APC toward the inactive form. This antagonism between APC and MPF generates two alternative states: APC active and cyclin B missing (G1-phase), or cyclin B present and APC inactive (S + G2 + M-phases). For the meta/anaphase transition, we proposed that APC is turned on by a hypothetical 'APC activating enzyme' (AAE). This enzyme is synthesized in an inactive form (apoAAE) as cells enter mitosis and must be activated to do its job. To account for indirect activation of APC by MPF, we assumed that high activity of MPF in mitosis favors the active form of AAE. Finally, to introduce the chromosome surveillance mechanism at the mitotic checkpoint, we assumed that, until all chromosomes are in tension on the metaphase plate, a strong phosphatase activity opposes MPF and keeps AAE inactive. Once the chromosomes are properly aligned, the phosphatase activity disappears, AAE switches to the active form, APC is activated and Cdc13 degraded. As the cell leaves M-phase, AAE also disappears, because its synthesis is MPF-dependent.

In this paper we combine this mitotic checkpoint mechanism with our previous models of G1 and G2 checkpoints to create, for the first time, a comprehensive model of the fission yeast cell cycle.

3. Mathematical model

Our mechanism (Fig. 2) encompasses the molecular interactions described in the previous section. The activity of Cdc13/Cdc2 is regulated by three sets of reactions. (1) Rum1 binding (lower right), which inhibits Cdc13/Cdc2 early in the cycle, plays a crucial role in the G1 checkpoint. (2) Tyr-15 phosphorylation (middle left), controlled by Wee1, Mik1 and Cdc25, arrests cells in G2. (3) Cdc13 degradation by the APC (top) is linked to chromosome alignment at metaphase through AAE synthesis and activation. We will show, by simulations, that the model can account reasonably well for the phenotypes of a large selection of mutant strains.

The mechanism is translated into a set of non-linear differential equations (Table 1) by standard principles of biochemical kinetics. A basal set of parameter values is given in Table 2. There are few direct kinetic measurements of the individual steps of the mechanism in fission yeast, so the parameters are chosen to fit the experimental data discussed below. Although it was no trivial matter to find these acceptable parameter values, most likely there exist other equally suitable parameter sets.

Some details of the mechanism deserve special attention.

- To keep the model as simple as possible (11 variables), we limit the mechanism to 'major players'. In particular, we ignore cyclins Cig1 and Cig2, i.e. all strains, including 'wild-type', actually refer to a *cig1*Δ *cig2*Δ genetic background. The phenotype of *cig1*Δ *cig2*Δ and true wild-type strains are similar, except that the double mutant has a slightly elongated G1-phase and is hyperfertile in conjugation [11]. In cells lacking both Cig1 and Cig2, oscillations of Cdc13 alone are sufficient to produce an ordered sequence of S- and M-phases [9]. It is this simplified system that we take as our 'baseline' or 'wild-type' cycle. Cig1 and Cig2 can be included in future elaborations of the model.
- In this model we assume that the reactions that regulate Cdc13/Cdc2 activity occur in the nucleus, where the dimers seem to be sequestered [38]. For this reason we write our differential equations in terms of nuclear concentrations of the various dimer forms. The rate of synthesis of Cdc13 is, therefore, multiplied by cell mass to take into account the accumulation of increasing quantities of Cdc13 in the nucleus as the cell grows. This effect couples cell growth to the CDK control

Table 1
Differential equations

Synthesis, degradation and interconversion of Cdc2/Cdc13 dimers and Rum1[a]

1. $\frac{d}{dt}[\text{Cdc2/Cdc13}] = k_1 \cdot \text{mass} - k_{wee}[\text{Cdc2/Cdc13}] + k_{cdc25}[\text{P-Cdc2/Cdc13}] - k_i[\text{Cdc2/Cdc13}][\text{Rum1}] + [\text{Rum1-Cdc2/Cdc13}](k_{ir} + k_4) - k_2[\text{Cdc2/Cdc13}]$

2. $\frac{d}{dt}[\text{P-Cdc2/Cdc13}] = k_{wee}[\text{Cdc2/Cdc13}] - k_{cdc25}[\text{P-Cdc2/Cdc13}] - k_2[\text{P-Cdc2/Cdc13}]$

3. $\frac{d}{dt}[\text{Rum1-Cdc2/Cdc13}] = k_i[\text{Rum1}][\text{Cdc2/Cdc13}] - [\text{Rum1-Cdc2/Cdc13}](k_4 + k_{2c} + k_{ir})$

4. $\frac{d}{dt}[\text{Rum1}] = k_3 - k_4[\text{Rum1}] - k_i[\text{Cdc2/Cdc13}][\text{Rum1}] + [\text{Rum1-Cdc2/Cdc13}](k_{ir} + k_{2c})$

Tyrosine phosphorylating/dephosphorylating enzymes[b]

5. $\frac{d}{dt}[\text{Cdc25P}] = \frac{k_{25}[\text{MPF}](1-[\text{Cdc25P}])}{J_{25} + 1 - [\text{Cdc25P}]} - \frac{k_{25r}[\text{Cdc25P}]}{J_{25r} + [\text{Cdc25P}]}$

6. $\frac{d}{dt}[\text{Wee1}] = \frac{k_{wr}(1-[\text{Wee1}])}{J_{wr} + 1 - [\text{Wee1}]} - \frac{k_w[\text{MPF}][\text{Wee1}]}{J_w + [\text{Wee1}]}$

7. $\frac{d}{dt}[\text{Mik1}] = \frac{k_{mr}(1-[\text{Mik1}])}{J_{mr} + 1 - [\text{Mik1}]} - \frac{k_m[\text{Mik1}]}{J_m + [\text{Mik1}]}$

Cyclin degradation pathway

8. $\frac{d}{dt}[\text{AAE}]_{total} = k_{as}[\text{MPF}] - k_{ad}[\text{AAE}]_{total}$

9. $\frac{d}{dt}[\text{AAE}] = (k_{aa}' + k_{aa}''[\text{MPF}])\frac{[\text{AAE}]_{total} - [\text{AAE}]}{J_{aa} + [\text{AAE}]_{total} - [\text{AAE}]} - \frac{k_{ai}[\text{AAE}]}{J_{ai} + [\text{AAE}]} - k_{ad}[\text{AAE}]$

10. $\frac{d}{dt}[\text{APC}] = (k_{apr}' + k_{apr}''[\text{AAE}])\frac{1-[\text{APC}]}{J_{apr} + 1 - [\text{APC}]} - k_{ap}([\text{Puc1}] \cdot \text{mass} + [\text{MPF}])\frac{[\text{APC}]}{J_{ap} + [\text{APC}]}$

Growth[c]

11. $\frac{d}{dt}\text{mass} = \mu \cdot \text{mass}$

Table 1 (*continued*)

Differential equations

Synthesis, degradation and interconversion of Cdc2/Cdc13 dimers and Rum1[a]

Rate functions

12. $k_2 = V_2' (1 - [APC]) + V_2'' [APC]$

13. $k_{2c} = V_{2c}' (1 - [APC]) + V_{2c}'' [APC]$

14. $k_4 = k_4' + k_4'' (Puc1 \cdot mass + [MPF])$

15. $k_{cdc25} = V_{25}' (1 - [Cdc25P]) + V_{25}'' [Cdc25P]$

16. $k_{wee} = V_{wee}' (1- [Wee1] + V_{wee}'' [Wee1] + V_{mik}' (1 - [Mik1]) + V_{mik}'' [Mik1]$

17. $k_{wr} = k_{wr}' + k_s$

18. $k_{25r} = k_{25r}' + k_s$

19. $k_{mr} = k_{mr}' + k_s$

20. $k_{ai} = k_{ai}' + k_x$

Auxiliary functions[d]

21. $[MPF] = [\text{B}] + \alpha[\text{P-B}]$

[a]For convenience, we sometimes use $[Cdc13]_{total} = [Cdc13/Cdc2] + [Cdc13/P\text{-}Cdc2] + [Trimer]$ and $[Rum1]_{total} = [Rum1] + [Trimer]$ as dynamic variables and calculate [Cdc13/P-Cdc2] and free [Rum1] from these conservation equations.
[b]To keep the model simpler, we assume that Wee1, Cdc25 and APC are present at a constant level, although this is certainly not true for Cdc25 [40]. The interested reader can find a model with fluctuating Cdc25 level in Ref. [5].
[c]We assume that mass $\rightarrow$ mass/2 whenever APC increases through 0.2.
[d]We assume that tyrosine phosphorylated Cdc13/Cdc2 dimers also have some H1 kinase activity [39], although much less than their dephosphorylated counterpart ($\alpha < 1$).

network, providing a mechanism for size control, as we shall see. At nuclear division (triggered by the activation of APC), the effective mass of the cell (mass per nucleus) decreases by a factor of two.

- As described earlier, we assume that CDK turns off the APC, and the APC destroys cyclin partners of CDK. Consequently, either APC is on and CDK activity is low (pre-Start), or APC is off and cyclin/Cdc2 dimers are plentiful (post-Start).
- There is also an antagonistic relationship between CDK and Rum1: Rum1 inhibits CDK activity [11,23,24], and CDK, by phosphorylating Rum1, promotes its degradation [47] Consequently, Rum1 is abundant in pre-Start and scarce in post-Start.
- We assume that Cdc13 gets degraded by APC from Cdc13/Cdc2/Rum1 trimers at a slower rate than from Cdc13/Cdc2 dimers ($k_{2c} < k_2$). That is, Rum1 not only inhibits Cdc13-dependent kinase activity, but also stabilizes Cdc13 against destruction by the APC, allowing a pool of inactive complexes to accumulate in G1-phase. This assumption is not a crucial part of the model.
- For simplicity (to have fewer differential equations) we assume that Rum1 only binds

to active Cdc13/Cdc2 dimers, but not to tyrosine-phosphorylated dimers.

- The CLN-type cyclin, Puc1, is present at constant low levels throughout the cell cycle. We assume that it accumulates in the nucleus (see 'Puc1 × mass' term), where it cooperates with MPF in phosphorylating Rum1 (both free and complexed with Cdc13/Cdc2) and in inactivating the APC. As we shall see, it plays an important role in the G1/S transition because its activity is perceptible during G1-phase in *cig1*Δ *cig2*Δ strains.
- We assume that apoAAE synthesis is stimulated by MPF activity, so that AAE protein will accumulate as cells enter M-phase and disappear when cells exit M-phase. In addition, conversion of apoAAE to the active form is assumed to depend on MPF activity. The second assumption is not absolutely necessary, but it makes the model considerably more robust.
- For simplicity, we use a primitive representation of the surveillance mechanisms for unreplicated DNA and unaligned chromosomes. We assume that, while DNA is being synthesized, there is an increased rate of dephosphorylation of Cdc25, Wee1 and Mik1 (expressed by parameter k_s in Table 1, Eq. (17) Eq. (18) Eq. (19)). Similarly, while chromosomes are in the process of condensation and alignment, we assume a large rate constant for inactivation of AAE (parameter k_x in Table 1, Eq. (20)).

4. The wild-type cell cycle

A simulation of 'wild-type' (*cig1*Δ *cig2*Δ) fission-yeast cell growth and division is shown in Fig. 3. The cell cycle should be viewed as an alternation between two characteristic phases: pre-Start (G1), when APC is active, Rum1 is present, and Cdc13 level is low, and post-Start (S + G2 + M), when APC is inactive, Rum1 is absent, and Cdc13 is accumulating. The parameters of the model are chosen so that the duration of pre-Start is short while the post-Start phase is long, as in wild-type fission yeast cells (Fig. 1A). In our simulation, the cell is so large in pre-Start that Cdc13/Cdc2, in combination with Puc1/Cdc2, quickly inactivates the APC and phosphorylates (destroys) Rum1. Rising CDK activity in the nucleus initiates DNA synthesis (the cell passes Start).

As Cdc13/Cdc2 dimers accumulate after Start, they are at first tyrosine phosphorylated by the unreplicated-DNA surveillance mechanism and by the cell-

Table 2
Parameter values[a]

Cyclin synthesis and degradation	
$k_1 = 0.03$	
$V_2' = 0.03$	$V_2'' = 1$
$V_{2c}' = 0.03$	$V_{2c}'' = 0.16$
AAE synthesis and degradation and APC regulation	
$k_{as} = 0.25$	$k_{ad} = 0.1$
$k_{aa}' = 0.001$	$k_{aa}'' = 1$
$k_{ai}' = 0.25$	$k_{ap} = 4$
$k_{apr}' = 0.04$	$k_{apr}'' = 3$
$J_{aa} = 0.1$	$J_{ai} = 0.1$
$J_{ap} = 0.01$	$J_{apr} = 0.01$
Rum1 synthesis and degradation and binding	
$k_3 = 0.15$	
$k_4' = 0.15$	$k_4'' = 20$
$k_i = 200$	$k_{ir} = 1$
Tyr-15 phosphorylation and dephosphorylation	
$V_{wee}' = 0.01$	$V_{wee}'' = 0.93$
$k_w = 0.5$	$k_{wr}' = 0.2$
$J_w = 0.2$	$J_{wr} = 0.2$
$V_{25}' = 0.01$	$V_{25}'' = 0.4$
$k_{25} = 0.5$	$k_{25r}' = 0.2$
$J_{25} = 0.2$	$J_{25r} = 0.2$
$V_{mik}' = 0.002$	$V_{mik}'' = 0.2$
$k_m = 0.1$	$k_{mr}' = 0$
$J_m = 0.2$	$J_{mr} = 0.2$
Thresholds	
Enter S-phase when APC = 0.2 (decreasing)	
Duration of S-phase = 12 min	
Enter M-phase when MPF = 0.2 (increasing)	
Exit M-phase when APC = 0.2 (increasing)	
Surveillance signals[b]	
$k_s = 0.5$ during S-phase, = 0 otherwise	
$k_x = 0, 1, 2, 3$[b]	
Miscellaneous	
$\mu = 0.005776\ \text{min}^{-1}$	(mass doubling time = 120 min)
$\alpha = 0.1$	Puc1 = 0.013

[a]The concentration variables are scaled so that all rate constants (*k*'s and *V*'s) have units of min^{-1} and all Michaelis constants (*J*'s) are dimensionless.

[b]k_x increases from 0 to 3 when cells enter mitosis, stays at 3 for 18 min as chromosomes condense and a mitotic spindle forms, and then decreases by 1 unit every 3 min as the three chromosomes align on the metaphase plate.

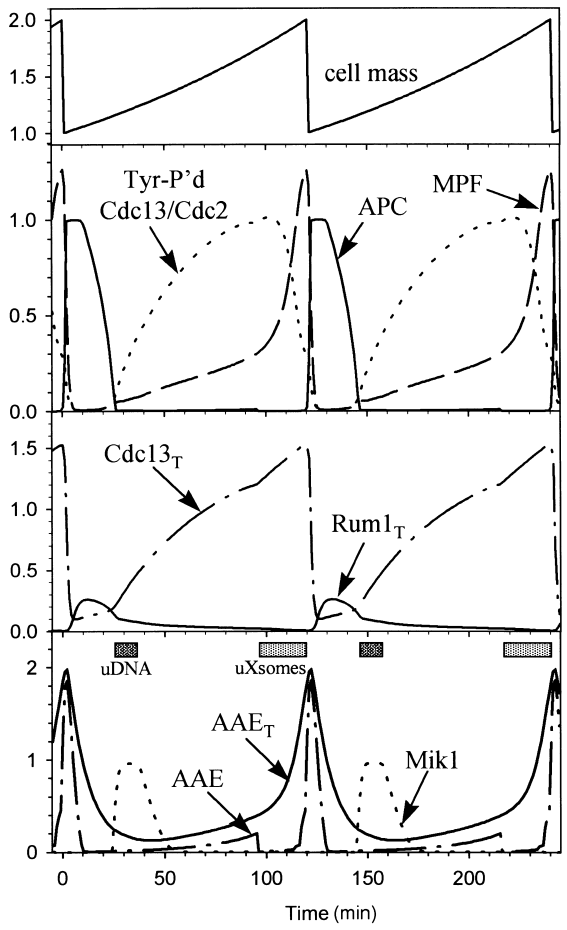

Fig. 3. Numerical simulation of the 'wild-type' (*cig1Δ cig2Δ*) cell cycle. The equations in Table 1, given the parameter values in Table 2, were solved using a fourth-order Runge–Kutta algorithm within the Time-Zero simulation program [45]. The rectangles in the bottom panel indicate the intervals when DNA is replicating (k_s = 0.5) and chromosomes are aligning (k_x = 3).

size surveillance mechanism. Under normal conditions, the DNA-replication requirement is satisfied long before the cell-growth requirement. When the cell grows large enough, the positive feedback loops activate the pool of preMPF (tyrosine-phosphorylated dimers), driving the cell into M-phase. G2-phase is long in wild-type strains because a cell must grow to this minimal size before it can enter mitosis [29]. In this manner, the rising pattern of Cdc13-dependent kinase activity can drive an orderly progression of S- and M-phases, if initiation of DNA synthesis requires a lower CDK activity than initiation of mitosis [9,41].

As MPF activity increases dramatically at the end of G2-phase, chromosomes begin to condense, a mitotic spindle forms, and apoAAE begins to accumulate. At the same time, dynamic microtubules search for kinetochores on individual chromosomes, which get pulled back and forth as they attach first to one pole of the spindle and then to the other. High MPF activity tries to activate AAE, but a strong signal coming from unaligned chromosomes (k_x = 3) inactivates AAE. As the chromosomes line up on the metaphase plate (and k_x drops to 0), MPF is able to activate AAE, which in turn activates APC. Cdc13 is degraded, AAE decays, and the cell returns to pre-Start.

4.1. Phase plane portraits

How size control at the G2 checkpoint operates in wild-type fission yeast is best explained with an (active MPF, total Cdc13) phase plane (Figs. 4 and 5). A phase plane portrait is a display of the MPF nullcline, where the rate of change of MPF activity equals zero, together with the cyclin nullcline, where the rate of cyclin synthesis is exactly balanced by its rate of degradation. The MPF nullcline is derived by setting to zero the right-hand-side of Eq. (1) of Table 1:

$$[\mathrm{Cdc13}]_{\mathrm{total}} = [\mathrm{MPF}]\left(1 + \frac{k_{wee} + k_2}{k_{cdc25}}\right) - \frac{k_1 \cdot mass}{k_{cdc25}}$$

assuming that $[\mathrm{Rum1}]_{\mathrm{total}}$ is small (which is certainly true in G2-phase, see Fig. 3). In deriving this equation, we have used the fact that [P-Cdc2/Cdc13] = $[\mathrm{Cdc13}]_{\mathrm{total}}$ − [MPF], assuming $\alpha = 0$. Furthermore, we assume that the regulatory enzymes (Cdc25, Wee1, Mik1, and APC) are all equilibrated between their active and inactive forms, and we treat mass and [AAE] as adjustable parameters. The cyclin nullcline,

$$[\mathrm{Cdc13}]_{\mathrm{total}} = \frac{k_1 \cdot mass}{k_2}$$

is derived under the same assumptions by adding Eqs. (1) and (2) of Table 1, and setting $(\mathrm{d}/\mathrm{d}t)[\mathrm{Cdc13}]_{total} = 0$.

The MPF nullcline (Fig. 4A) is N-shaped because of the positive feedback loops in the MPF activation process. At low cyclin levels, most dimers are tyrosine-phosphorylated and inactive, whereas at high cyclin levels, most dimers are not phosphorylated

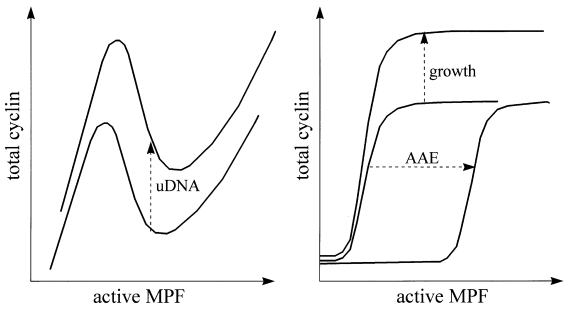

Fig. 4. Schematic diagrams of the nullclines in the (MPF, total Cdc13) phase plane. (A) MPF nullcline, where the rate of production of active MPF is exactly balanced by its rate of removal. The MPF nullcline is shifted up in the presence of unreplicated DNA. (B) Cyclin nullcline, where the rate of cyclin synthesis is exactly balanced by its rate of degradation (both free cyclin and complexed forms). The cyclin nullcline is shifted up by growth and to the right by AAE.

and active. At intermediate cyclin levels, there exists a branch of unstable steady states (with negative slope), where the fraction of tyrosine-phosphorylated dimers is dropping rapidly with increasing MPF activity (see Fig. 3B of Ref. [46]). The location of the MPF nullcline is especially sensitive to unreplicated DNA, which makes it harder for MPF to turn on the positive feedback loops.

The cyclin nullcline (Fig. 4B) is sigmoid-shaped because MPF inactivates APC: at low MPF activity, APC is active, so the total cyclin level is low, whereas at high MPF activity, APC is inactive and cyclin is plentiful. The MPF activity at which the APC turns off depends on the amount of active AAE in the cell: in late G1, when AAE is scarce, only a little MPF activity is needed to inactivate APC, whereas in metaphase, when active AAE is plentiful, even high MPF activity cannot keep APC inactive. Notice that the entire cyclin nullcline moves up (to higher cyclin levels) as the cell grows, because Cdc13/Cdc2 dimers are accumulating in the nucleus.

When cells are in S-phase with unreplicated DNA,

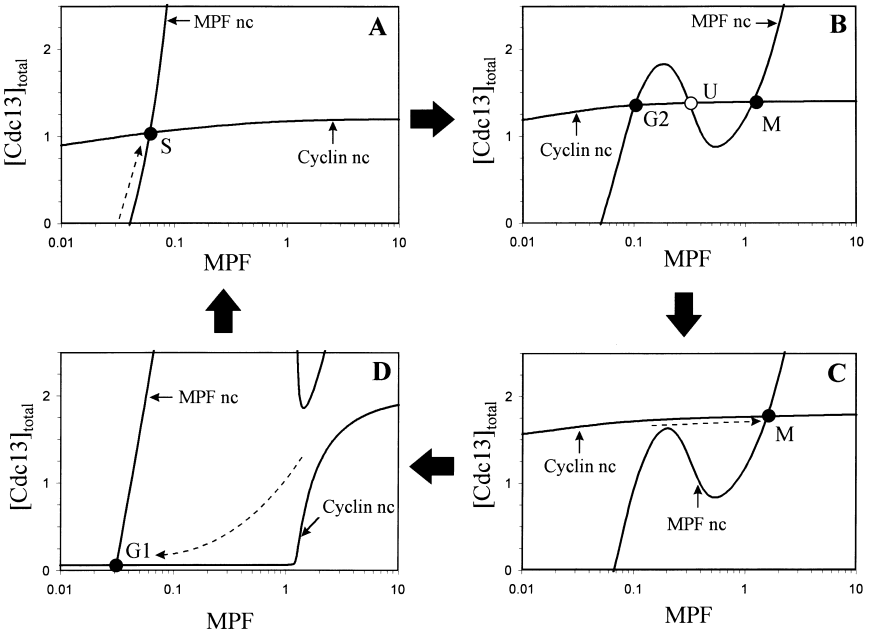

Fig. 5. Phase plane portraits of the wild-type control system. Solid lines are nullclines; dashed lines are representative trajectories. (A) S-phase: the MPF nullcline is steep and not N-shaped, because unreplicated DNA activates the phosphatases working on Wee1, Mik1 and Cdc25, thereby abolishing the positive feedback loops. The control system halts at the only stable steady state (S), which has low MPF activity. (B) G2-phase: for those cells which have finished DNA synthesis, the control system has two stable steady states (G2 and M). Accumulation of Cdc13/Cdc2 dimers in the nucleus, as cells grow, pulls the cyclin nullcline up. (C) M-phase: when cells reach the critical size for mitosis, the G2 steady state is annihilated by a saddle-node bifurcation. (D) G1-phase: at the meta/anaphase transition, APC is activated, the cyclin nullcline collapses, and the control system must move from M to G1, where it arrests for only a short time while Rum1 is high. But newborn cells are so large that Rum1 is quickly phosphorylated and destroyed, returning the phase plane portrait to (A).

the maximum of the MPF nullcline will be very high. On the other hand, the cyclin nullcline steps up at very low MPF activity, because there is little AAE around. The two balance curves intersect at a single steady state (S) with a high cyclin level and low MPF activity (Fig. 5A). In this steady state, most dimers are kept in the less active, tyrosine-phosphorylated form. Presumably, there is enough Cdc2 kinase activity (even though most of the dimers are tyrosine-phosphorylated) to drive the cell through S-phase, but not into M-phase.

In early G2-phase, the MPF nullcline drops (as the effects of unreplicated DNA disappear), and the two nullclines now intersect at three possible steady states (Fig. 5B). All three steady states (G2, U and M) have high cyclin level (because APC is off). G2 has little MPF activity, whereas M has a high MPF activity. G2

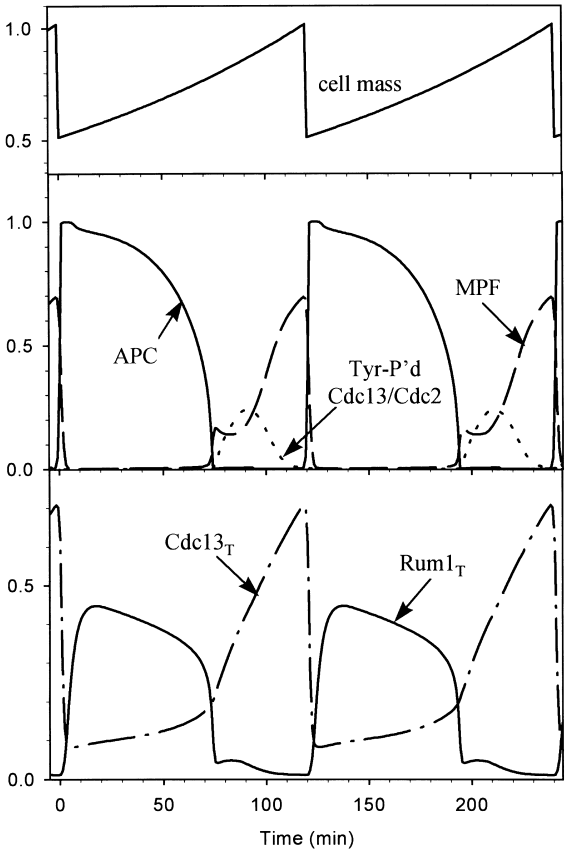

Fig. 6. Numerical simulation of the *wee1*⁻ cell cycle in a *cig1*Δ *cig2*Δ genetic background. Parameter values as in Table 2, except $V_{wee}' = V_{wee}'' = 0$.

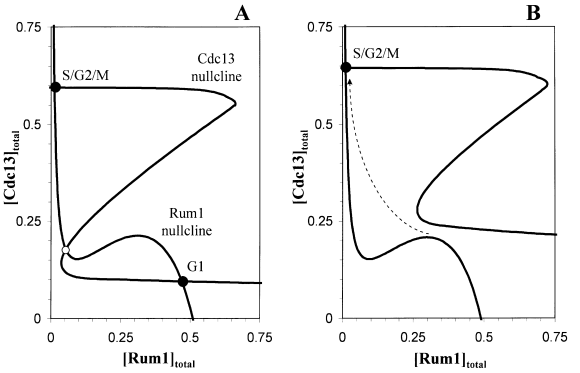

Fig. 7. Phase plane portraits of the Start control system. Solid lines are nullclines; dashed lines are representative trajectories. (A) pre-Start: three steady states. (B) post Start. As cells grow, the nullclines shift and the G1 steady state is lost by a saddle-node bifurcation; thereafter, cells are attracted to the steady state (S + G2 + M) with high Cdc13 level and little Rum1.

and M are stable nodes; U is an unstable 'saddle point'. The U and M states are introduced by a saddle-node bifurcation as DNA replication finishes, but the control system remains in the G2 steady state with low MPF activity (which is merely a continuation of the S state of Fig. 5A).[1]

As the cell grows, the cyclin nullcline continues to move up, as more and more Cdc13/Cdc2 complexes accumulate in the nucleus. When the cell reaches a critical mass, G2 disappears by fusing with U, and the only remaining attractor is now M (Fig. 5C). At this time, cells start to dephosphorylate Cdc13/Cdc2 dimers and move toward the mitotic state.

When the chromosomes are properly aligned on the metaphase plate, AAE is activated and the APC turns on. At this stage MPF activity must be very large to turn off the APC, because it is opposed by lots of active AAE, so the step-up in the cyclin nullcline moves to a large MPF value. At the same time, the MPF nullcline moves up dramatically because APC is now turned on. As a result of these movements of the nullclines, the mitotic state (M) disappears, and the cell proceeds toward a G1 steady state (Fig. 5D).

Very soon, however, Cdc13-dependent kinase, with the help of the Rum1-insensitive Puc1-dependent

[1] Our model suggests that the cell cycle control system of fission yeast shows bistability in G2-phase. There is no direct experimental evidence for this bistability, but it gives an interesting interpretation of classical nutritional-shift experiments [27] (for more details see Ref. [5]).

kinase, turns off the APC, and the nullclines regain their positions in Fig. 5A, as the cell enters S-phase.

In wild-type fission yeast, size control operates at the G2 checkpoint. Cells leaving mitosis are large enough to satisfy the size requirement of the G1 checkpoint, so the G1 size control is cryptic. However, by decreasing the Wee1/Cdc25 ratio, we can lower the maximum of the MPF nullcline and decrease the size at which the G2 steady state is abolished. Such mutant cells (either *wee1*$^-$ or *cdc25*^{op}), which divide at a smaller size, can now reveal the operation of a size control in G1-phase [17,28].

5. The cell cycle of wee1$^-$ mutants

A numerical simulation of *wee1*$^-$ *cig1*Δ *cig2*Δ is shown in Fig. 6. The alternation of APC activity and Cdc13 level is still observable, but G1-phase, when APC is active and Rum1 level is high, is much longer than in wild-type. After the G1/S transition, Cdc13 accumulates as in wild-type, but MPF gets activated much faster because it cannot be efficiently phosphorylated on Tyr-15. Consequently, G2-phase is much shorter and cells divide at a reduced size.

5.1. Phase plane portraits

To illustrate how *wee1*$^-$ cells coordinate growth and division at the G1 checkpoint, we use phase planes (Fig. 7) to represent the interactions between Rum1 and Cdc13, which are crucial for triggering the G1/S transition. (Equations for these nullclines are derived in the Appendix of Ref. [37]). The Rum1 nullcline is N-shaped because Rum1 and Cdc13 are competing for dominance: Rum1 is inhibiting Cdc13/Cdc2, while Cdc13/Cdc2 is phosphorylating Rum1 and making it unstable. When Cdc13/Cdc2 activity is high, then the Rum1 steady state level is low (left branch of the Rum1 nullcline) and vice versa. The N-shape of the Cdc13 nullcline derives from the mutual inhibitory effects of Cdc13 and APC, and the synergistic effects of Rum1 and APC. When Rum1 is low, the APC is off, so Cdc13-dependent kinase is plentiful and active (top branch of the Cdc13 nullcline); when Rum1 is dominant, the APC is on, so Cdc13-dependent kinase is scarce and inactive (bottom branch of the Cdc13 nullcline).

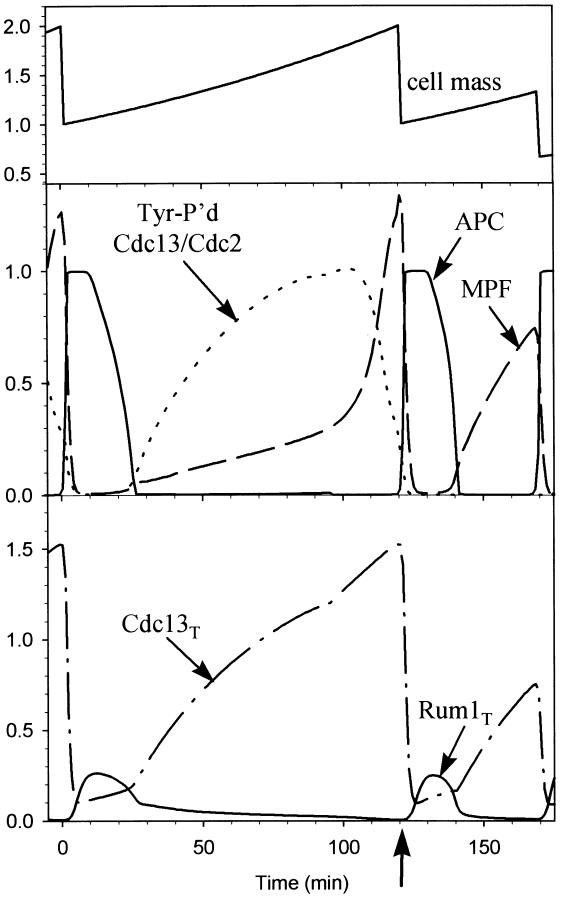

Fig. 8. Numerical simulation of the mitotic catastrophe in *wee1*$^-$ *mik1*Δ cells in a *cig1*Δ *cig2*Δ genetic background. To the left of the arrow: one cycle of a *wee1*$^+$ *mik1*Δ cell, parameter values as in Table 2, except $V_{mik}' = V_{mik}'' = 0$. At the arrow the cells are 'raised to the non-permissive temperature', i.e. we set $V_{wee}' = V_{we}'' = 0$. MPF activity at the 'non-permissive temperature' rises so fast that mitosis is initiated before DNA replication can be completed.

The stable steady state on the right branch of the Rum1 nullcline corresponds to a G1 state (pre-Start) of the cell cycle: Rum1 level is high and Cdc13 low. Since total Rum1 exceeds total Cdc13, most Cdc13 is sequestered as inactive trimers, and APC is on. The stable steady state on the left branch of the Rum1 nullcline corresponds to an S + G2 + M state (post-Start) of the cell cycle: Cdc13 level is high and Rum1 low. In this state most Cdc13 is in functional dimers, and APC is inactive.

At birth, a cell finds itself at the stable G1 state. As it grows, the nullclines shift positions: the Cdc13 null-

Table 3
Cell cycle properties of mutant strains (in a *cig1*Δ *cig2*Δ genetic background)

Strain	Mass at birth	Mass at start	G1[a]	S + G2 + M[a]
'wild-type'	1	1.11	18	102
	Spore[b]	0.76		163
*rum1*Δ	0.99	1.08	15	105
	Spore	0.44		255
wee1$^-$	0.51	0.75	67	53
	Spore	0.75		54
wee1$^-$ *mik1*Δ	0.46[c]	0.75	85	35
	Spore	0.74		36
wee1$^-$ *rum1*Δ	0.24[c]	0.31	42	78
	Spore	0.32		77
*puc1*Δ	1.36	1.99	66	54
	Spore	2.00		54
*puc1*Δ *rum1*Δ	1.03	1.20	26	94
	Spore	0.78		158
*puc1*Δ *wee1*$^-$	1.07	1.83	93	27
	Spore	1.82		29
*puc1*Δ *wee1*$^-$ *rum1*Δ	0.31[c]	0.43	55	65
	Spore	0.46		63

[a]Duration (in min) of G1-phase and S + G2 + M-phases.
[b]Spore germination (simulation started at a very small size) reveals the true minimal size for Start.
[c]These strains are too small at birth to be viable. We report what the cell cycle properties would be if the strain were viable.

cline moves up as more of it accumulates in the nucleus, the Rum1 nullcline moves down as it is phosphorylated by the accumulating CDK activity and degraded. Eventually, at a critical size, the G1 state is lost by a saddle-node bifurcation (fusing with the unstable saddle point). Thereafter, the control system moves to the only stable steady state, S + G2 + M.

6. Two catastrophes

Although *wee1*$^-$ mutants enter mitosis at a reduced size (because the size requirement of the G2 checkpoint has been abolished), they never enter into mitosis in the presence of unreplicated DNA [42]. The S-M coupling mechanism is still intact because MPF activity can still be suppressed by Mik1 in response to unreplicated DNA. Mik1 is not an essential gene in wild-type [16], but it plays a crucial role in *wee1*$^-$ cells, where it is the only tyrosine kinase to keep MPF temporarily inactive after Start. This is illustrated in Fig. 8, a simulation of the consequences of knocking out both *mik1* and *wee1*. Since there is no tyrosine kinase to inactivate MPF, all Cdc13/Cdc2 dimers (which accumulate rapidly after APC is switched off at Start) are active, and the abruptly rising MPF activity initiates chromosome condensation before DNA replication can be finished. Presumably condensed chromosomes cannot complete their replication, but, as long as their kinetochores are replicated, they can still align on the metaphase plate. In that case, AAE will activate, APC will turn on, and chromatid separation will commence but, of course, cannot be completed. As the septum is laid down, the unreplicated DNA is cut in random pieces, producing inviable aneuploid cells. This 'cut' phenotype, caused by premature initiation of mitosis, is called mitotic catastrophe [17].

A different kind of catastrophe results from knocking out both *rum1* and *wee1*. Although deletion of *rum1* results in no apparent phenotype in wild-type background, it causes a dramatic reduction in size of *wee1*$^-$ cells that causes a loss of viability [22] (see Table 3). This observation suggests that, in the absence of Rum1 and Wee1, fission yeast cells lose size control at both G1 and G2 checkpoints [22, 43].

In our model there are two distinct mechanisms for

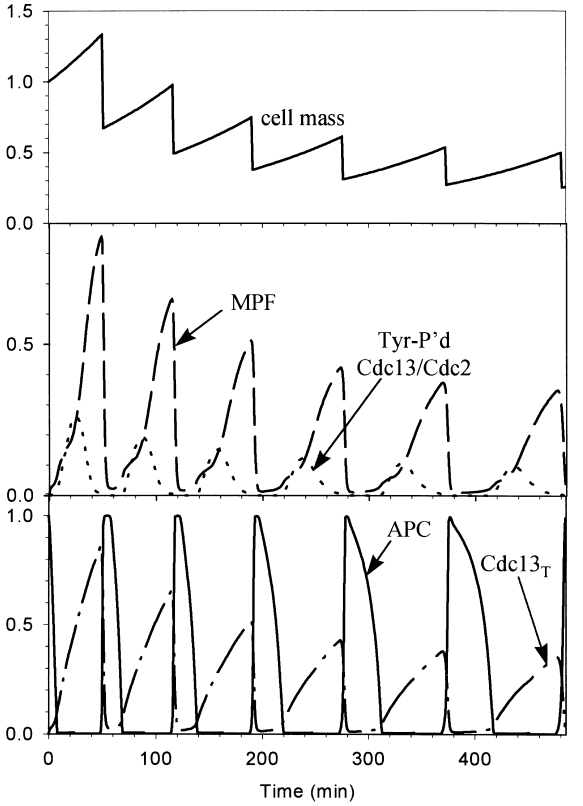

Fig. 9. Numerical simulation of catastrophic divisions in *wee1*$^-$ *rum1*Δ cells in a *cig1*Δ *cig2*Δ genetic background. Parameter values as in Table 2, except $V_{wee}' = V_{wee}'' = k_3 = 0$. Initial conditions: division of a *wee1*$^+$ *rum1*Δ cell. In the double mutant cell, the division cycle runs faster than the growth cycle, and cells get smaller and smaller at each division. Eventually this simulation settles onto a balanced cycle of growth and division, with a birth size of 1.7 μm, which is probably too small for viability.

size control at the G1 checkpoint, relying on the antagonistic relations between Rum1 and CDK and between APC and CDK. With the parameter values we have chosen, the APC–CDK size requirement is cryptic, i.e. it is satisfied at a smaller size than the Rum1–CDK size requirement. But, if the Rum1–CDK interaction is knocked out (*rum1*Δ), then the underlying APC–CDK size requirement is revealed. Indeed, this mutant strain (*wee1*$^-$ *rum1*Δ *cig1*Δ *cig2*Δ) should be comparable with the hypothetical 'primitive eukaryotic cell' described in [37,44], which relies on the interaction between APC and CDK to coordinate growth and division.

The simulation in Fig. 9 shows that *wee1*$^-$ *rum1*Δ cells decrease in size to about 3.5 μm at division (1/4 the size of wild-type cells), where they execute balanced growth and division, coordinated by a size requirement for inactivating the APC at the G1/S transition. Although balanced growth is possible in the mathematical model, *wee1*$^-$ *rum1*Δ cells are actually inviable. Perhaps fission yeast cells of such small size are unable to survive for other reasons.

7. The role of starter kinase, Puc1

Because our model is designed for *cig1*Δ *cig2*Δ strains, Puc1 plays a major role as a starter kinase phosphorylating Rum1 and inactivating APC at the G1/S transition. If Puc1 is missing, then Cdc13 must do these jobs alone. Since Cdc13/Cdc2 complexes are inhibited by Rum1 in G1-phase, the G1/S transition will be greatly delayed. This is shown

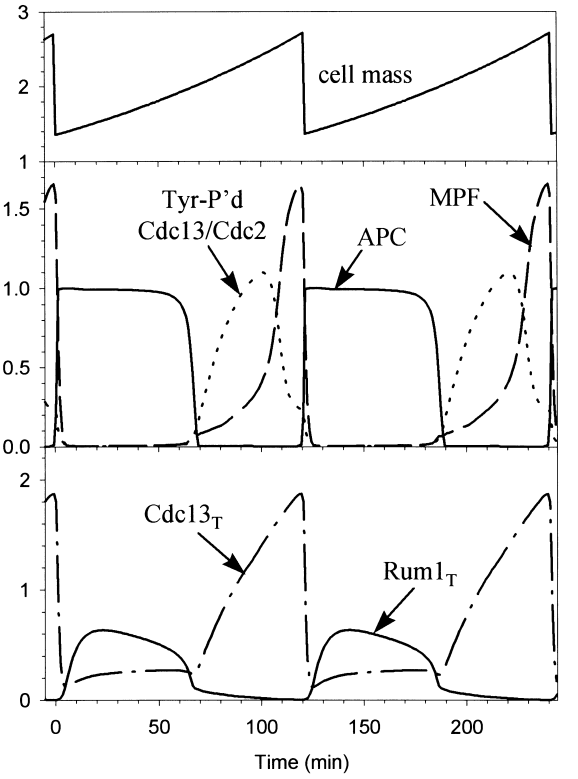

Fig. 10. Numerical simulation of the cell cycle in *puc1*$^-$ *cig1*Δ *cig2*Δ. Parameter values as in Table 2, except *Puc1* = 0. These cells execute Start at an unusually large size because they lack starter kinase. The G2 size requirement is operational but cryptic.

on Fig. 10, a simulation of the triple deletion *puc1*Δ *cig1*Δ *cig2*Δ. This strain has a long G1-phase and divides at 19 μm (about 35% larger than wild-type). The coordination of growth and division occurs at the G1 checkpoint, but the minimal size for the G1/S transition is larger than the size requirement at the G2 checkpoint. Hence, the G2 size control is cryptic, as suggested by the short G2-phase. Although a description of this triple cyclin deletion strain has not yet appeared, preliminary reports (S. Moreno, personal communication) are in accord with our model.

We can predict the phenotypes of other multiple-mutant strains that have yet to be constructed and analyzed (see Table 3) (unless stated otherwise, comparisons are made to *puc1*Δ *cig1*Δ *cig2*Δ).

- *puc1*Δ *rum1*Δ *cig1*Δ *cig2*Δ. Without Rum1, Cdc13-dependent kinase is more active in G1-phase but there is less of it. Start is now controlled by the interaction between Cdc13/Cdc2 and APC, and the minimal size for the G1/S transition (as revealed by spore germination) has been reduced from 2 to 0.78. In cycling cells, the G1 size requirement is cryptic; growth and division are coordinated by the G2 checkpoint, so the mutant cells are nearly the same size as wild-type. Other parameter values may predict different sizes at Start: mutant cells may be larger than wild-type, but they may never be smaller because the normal G2 size control is still in place.
- *puc1*Δ *wee1*$^-$ *cig1*Δ *cig2*Δ Without Wee1, the duration of G2-phase is shorter and the size at Start is smaller. Notice that, when Cdc13 is the only cyclin around, Wee1 has a noticeable effect on size at Start because it inhibits the little bit of Cdc13-dependent kinase activity present in G1-phase. In the absence of Wee1, Cdc13/Cdc2 is more active and cells enter S-phase at a smaller size. Also, since G2-phase is shorter, size at division is considerably smaller.
- *puc1*Δ *wee1*$^-$ *rum1*Δ *cig1*Δ *cig2*Δ. These cells are larger at division than *puc1*$^+$ *wee1*$^-$ *rum1*Δ *cig1*Δ *cig2*Δ because Cdc13/Cdc2 alone must turn off APC, but they are still very small and probably inviable.

8. Conclusion

We have presented a simple yet comprehensive model of the fission yeast cell cycle (*cig1*Δ *cig2*Δ) with all three checkpoints in place. The G1/S transition is governed by interactions of Cdc13/Cdc2 with Rum1 and the APC, the G2/M transition by tyrosine phosphorylation of Cdc2, and the meta/anaphase transition by a hypothetical 'APC activating enzyme' (AAE). In this mechanism, there are three opportunities to check cell size. The largest size requirement controls the G2/M transition in wild-type fission yeast cells; it is driven by the interplay of cyclin accumulation (growth related) and the positive feedback of MPF activity on Wee1 and Cdc25. When this requirement is eliminated (by *wee1*$^-$ or *cdc25*^{op} mutation), the next smaller size requirement takes control of the G1/S transition; it is driven by the antagonistic interactions of Rum1 and Cdc13/Cdc2. When both requirements are lifted (in the *wee1*$^-$ *rum1*Δ strain), the smallest size requirement is revealed: a control of the G1/S transition by the growth-regulated competition between APC and Cdc13/Cdc2. The third and smallest size requirement is apparently below the limit of viability of modern fission yeast, but it is thought to represent the original size control of the earliest eukaryotic cells [37].

To our knowledge, this is the first realistic model of all three cell cycle checkpoints in a living eukaryote. The model is consistent with observed phenotypes of many relevant mutant strains of fission yeast, and it predicts interesting phenotypes for some multiple-mutant strains that have not yet been constructed and analyzed (Table 3).

The model is constructed for fission yeast *cig1*Δ *cig2*Δ double-mutant cells, which are similar to wild-type cells in all respects except mating efficiency (the mutants are hyperfertile). It could easily be expanded to *cig1*Δ *cig2*$^+$ strains by adding a few more variables representing Cig2-dependent kinase, which plays a role in G1- and S-phases of the cycle. It has not escaped our attention that this expanded

model, with ‘G1’ and ‘G2’ cyclins and three checkpoints, provides a good starting point for modeling the mammalian cell cycle. Only the names of the variables need be changed.

Acknowledgements

Our research is supported by the National Science Foundations of the USA (MCB-9600536) and Hungary (T-022182 and FKFP 0350), and the Howard Hughes Medical Institute (75195-542501).

References

[1] B. Alberts, D. Bray, J. Lewis, M. Raff, K. Roberts, J.D. Watson, Molecular Biology of the Cell, Garland, New York, 1994.
[2] A. Goldbeter, Proc. Natl. Acad. Sci. USA 88 (1991) 9107.
[3] J.J. Tyson, Proc. Natl. Acad. Sci. USA 88 (1991) 7328.
[4] B. Novak, J.J. Tyson, J. Theor. Biol. 165 (1993) 101.
[5] B. Novak, J. Tyson, J. Theor. Biol. 173 (1995) 283.
[6] C.D. Thron, Biophys. Chem. 57 (1996) 239.
[7] J. Hayles, P. Nurse, Annu. Rev. Genet. 26 (1992) 373.
[8] D. Fisher, P. Nurse, Sem. Cell Biol. 6 (1995) 73.
[9] D. Fisher, P. Nurse, EMBO J. 15 (1996) 850.
[10] S. Moreno, J. Hayles, P. Nurse, Cell 58 (1989) 361.
[11] C. Martin-Castellanos, K. Labib, S. Moreno, EMBO J. 15 (1996) 839.
[12] O. Mondesert, C. McGowan, P. Russell, Mol. Cell. Biol. 16 (1996) 1527.
[13] G. Basi, G. Draetta, Mol. Cell. Biol. 15 (1995) 2028.
[14] U. Fleig, K. Gould, Sem. Cell Biol. 2 (1991) 195.
[15] P. Russell, P. Nurse, Cell 49 (1987) 559.
[16] K. Lundgren, N. Walworth, R. Booher, M. Dembski, M. Kirschner, D. Beach, Cell 64 (1991) 1111.
[17] P. Russell, P. Nurse, Cell 45 (1986) 145.
[18] J. Millar, C. McGowan, G. Lenaers, R. Jones, P. Russell, EMBO J. 10 (1991) 4301.
[19] T. Coleman, W. Dunphy, Curr. Opin. Cell Biol. 6 (1994) 877.
[20] R. Kovelman, P. Russell, Mol. Cell. Biol. 16 (1996) 86.
[21] R. Aligue, L. Wu, P. Russell, J. Biol. Chem. 272 (1997) 13320.
[22] S. Moreno, P. Nurse, Nature 367 (1994) 236.
[23] J. Correa-Bordes, P. Nurse, Cell 83 (1995) 1001.
[24] P.V. Jallepalli, T.J. Kelly, Genes Dev. 10 (1996) 541.
[25] P. Nurse, Phil. Trans. R. Soc. Lond., Ser. B 332 (1991) 271.
[26] P.A. Fantes, J. Cell Sci. 24 (1977) 51.
[27] P. Fantes, P. Nurse, Exp. Cell Res. 107 (1977) 377.
[28] P. Nurse, Nature 256 (1975) 457.
[29] P. Nurse, P.A. Fantes, in: P.C.L. John (Ed.), The Cell Cycle, Cambridge University Press, Cambridge, 1981, p. 85.
[30] B. Novak, J.J. Tyson, Proc. Natl. Acad. Sci. USA 94 (1997) 9147.
[31] A. Murray, Cell 81 (1995) 149.
[32] M.-A. Felix, J.-C. Labbe, M. Doree, T. Hunt, E. Karsenti, Nature 346 (1990) 379.
[33] A. Amon, S. Irniger, K. Nasmyth, Cell 77 (1994) 1037.
[34] H. Funabiki, H. Yamano, K. Kumada, K. Nagao, T. Hunt, M. Yanagida, Nature 381 (1996) 438.
[35] A. Amon, EMBO J. 16 (1997) 2693.
[36] J. Minshull, H. Sun, N. Tonks, A. Murray, Cell 79 (1994) 475.
[37] B. Novak, A. Csikasz-Nagy, B. Gyorffy, K. Nasmyth, J.J. Tyson, Phil. Trans. R. Soc. Lond., Ser. B. (1997) (submitted).
[38] I. Gallagher, C. Alfa, J. Hyams, Mol. Biol. Cell. 4 (1993) 1087.
[39] A. Borgne, L. Meijer, J. Biol. Chem. 271 (1996) 27847.
[40] S. Moreno, P. Nurse, P. Russell, Nature 344 (1990) 549.
[41] B. Stern, P. Nurse, Trend. Genet. 12 (1996) 345.
[42] T. Enoch, P. Nurse, Cell 60 (1990) 665.
[43] A. Sveiczer, B. Novak, J. Mitchison, J. Cell Sci. 109 (Pt. 12) (1996) 2947.
[44] K. Nasmyth, Phil. Trans. R. Soc. Lond., Ser. B. 349 (1995) 271.
[45] T.B. Kirchner, Time-Zero The Integrated Modeling Environment, Version 2, Quaternary Software, Fort Collins, CO, 1990.
[46] B. Novak, J.J. Tyson, J. Cell Sci. 106 (1993) 1153.
[47] J. Benito, C. Martin-Castellanos, S. Moreno, EMBO J. 17 (1998) 482.